ELSEVIER

CrossMark

Data Article

Data on a new beta titanium alloy system reinforced with superlattice intermetallic precipitates

Alexander J. Knowles [a,b,*], Tea-Sung Jun [a,c], Ayan Bhowmik [a],
Nicholas G. Jones [b], T. Ben Britton [a], Finn Giuliani [a],
Howard J. Stone [b], David Dye [a]

[a] Department of Materials, Imperial College, South Kensington, London SW7 2AZ, UK
[b] Department of Materials Science and Metallurgy, University of Cambridge, Cambridge CB3 0F3, UK
[c] Department of Mechanical Engineering, Incheon National University, 119 Academy-ro, Yeonsu-go, Incheon
22012, South Korea

ARTICLE INFO

ABSTRACT

The data presented in this article are related to the research article entitled "a new beta titanium alloy system reinforced with superlattice intermetallic precipitates" (Knowles et al., 2018) [1]. This includes data from the as-cast alloy obtained using scanning electron microscopy (SEM) and x-ray diffraction (XRD) as well as SEM data in the solution heat treated condition. Transmission electron microscopy (TEM) selected area diffraction patterns (SADPs) are included from the alloy in the solution heat treated condition, as well as the aged condition that contained $< 100\,nm$ B2 TiFe precipitates [1], the latter of which was found to exhibit double diffraction owing to the precipitate and matrix channels being of a similar width to the foil thickness (Williams and Carter, 2009) [2]. Further details are provided on the macroscopic compression testing of small scale cylinders. Of the micropillar deformation experiment performed in [1], SEM micrographs of focused ion beam (FIB) prepared $2\,\mu m$ micropillars are presented alongside

those obtained at the end of the in-situ SEM deformation as well as videos of the in-situ deformation. Further, a table is included that lists the Schmidt factors of all the possible slip systems given the crystal orientations and loading axis of the deformed micropillars in the solution heat treated and aged conditions.

Specifications Table

Subject area	Materials Science
More specific subject area	*Metallurgy, Titanium Alloys*
Type of data	*Images (microscopy: SEM, TEM), graph (XRD, load-displacement), Table (compression test data, Schmidt factors), video (in-situ SEM)*
How data was acquired	*SEM Zeiss Auriga & FEI Quanta, FIB-SEM FEI Helios, TEM JEOL 2100F*
Data format	*Analysed*
Experimental factors	Arc melted Ti-17Fe-23Mo alloy, solution heat treated at 1170 °C for 16 h, followed by an aging heat treatment at 750 °C for 80 h
Experimental features	*The solution heat treatment resulted in a single phase bcc microstructure, while the aging heat treatment produced a nanoscale lamellar microstructure of a bcc (Ti, Mo) matrix with B2 TiFe precipitates.*
Data source location	*Department of Materials, Imperial College, South Kensington, London SW7 2AZ, UK*
	Department of Materials Science and Metallurgy, University of Cambridge, Cambridge, CB3 0F3, UK
Data accessibility	*Data is with this article and* [1]

Value of the data

- Details of dendritic segregation that occurs within the Ti–Fe–Mo alloy produced under arc melting and the ability to form a homogeneous microstructure following solution heat treatment.
- Details of double diffraction occurring in the aged alloy owing to its two-phase lamellar microstructure being of a similar length scale to the foil thickness, ~100 nm.
- Details of the 2 μm micropillar deformation of the Ti–Fe–Mo alloy.

1. Data

The data we report here were obtained from a new Ti–17Fe–23Mo alloy [1]. This alloy was designed so as to be solution heat treatable within the bcc (A2) single phase field, and, following an aging heat treatment, to form nanoscale B2 TiFe intermetallic precipitates from within the A2 matrix. Here, further details of the as-cast microstructure from scanning electron microscopy (SEM) and x-ray diffraction (XRD) are presented as well as Transmission electron microscopy (TEM) selected area diffraction patterns (SADPs) and mechanical testing details of small scale macro-compression testing and micropillar deformation in the solution heat treatment and aged conditions.
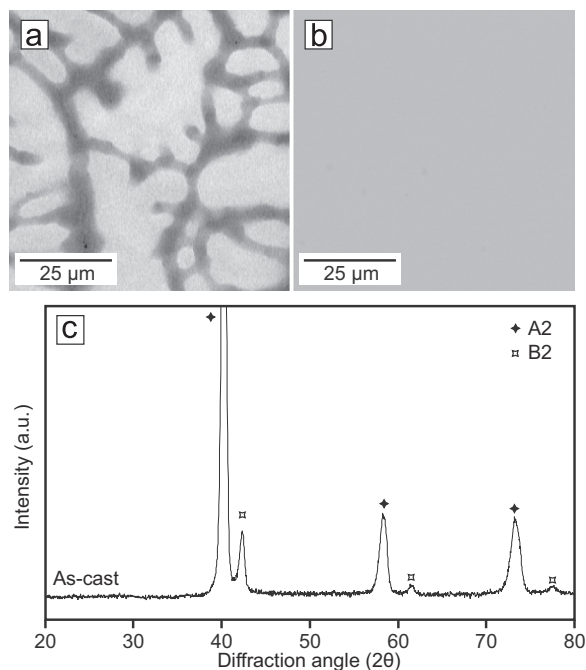
Fig. 1. Microstructure of the alloy observed by SEM BSE in (a) the as-cast and (b) the solution heat treated conditions, as well as (c) an XRD pattern collected in the as-cast condition (Cu Kα).
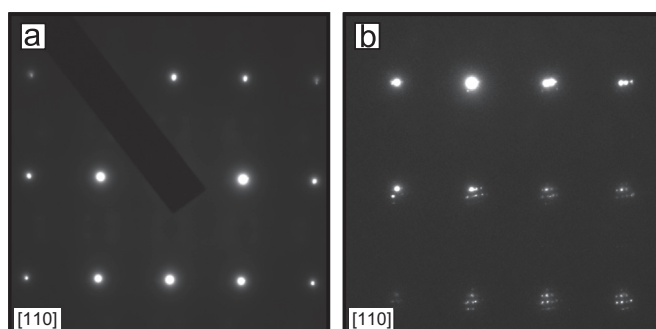

Fig. 2. TEM SAPDs from the alloy in (a) the solution heat treated and (b) aged conditions (please note beam stop in (a)).

2. Experimental design, materials and methods

Full details of the alloy preparation can be found in [1]. The Ti–17Fe–23Mo alloy was produced by arc melting > 99.9 at% purity elements under an argon atmosphere. Sections of this ingot were encapsulated within quartz ampoules under argon and solution heat treated at 1170 °C for 16 h followed by an aging heat treatment at 750 °C for 80 h, with the samples water quenched and studied after each heat treatment.

Scanning electron microscopy (SEM) was performed using a Zeiss Auriga operated at 20 kV. While x-ray diffraction (XRD) data was collected with Bruker D8 diffractometer using Cu Kα radiation on flat samples.

~8 mm in diameter. Foils of the alloy for transmission electron microscopy (TEM) were prepared by electropolishing according to [1]. These were then studied using a JEOL 2100F microscope.
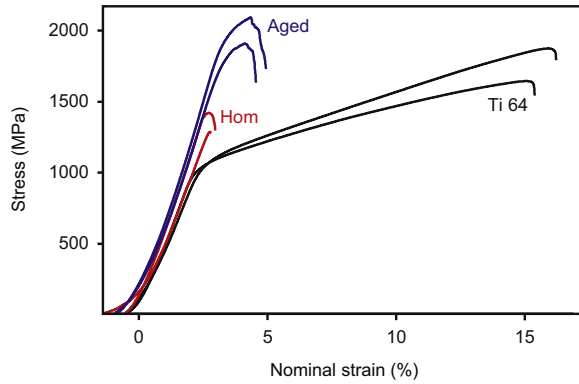
Fig. 3. Compression stress strain curves for the Ti–Fe–Mo alloy in the solution heat treated and aged conditions as well as a Ti-64 reference sample.

Table 1
Modulus, yield strength, 0.2% proof strength and compressive strain to failure of the Ti–Fe–Mo alloy in the solution heat treated and aged conditions, in addition to a Ti-64 reference sample.

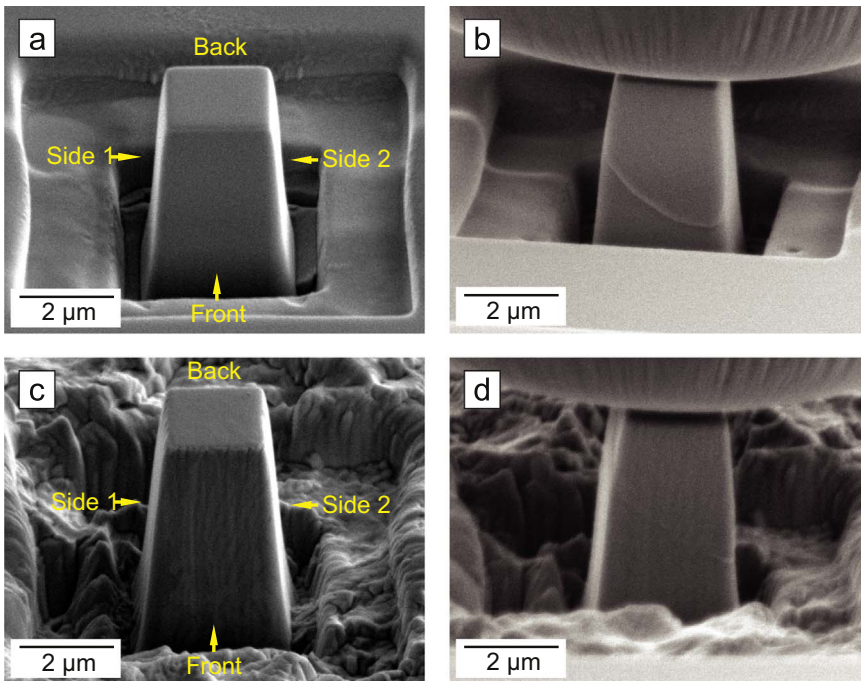| Alloy	Modulus (GPa)	Proof stress, 0.2% (MPa)	Strain to failure (%)
Ti–Fe–Mo Soln.	–	1335 ± 85	2.9 ± 0.1
Ti–Fe–Mo Aged	139	1890 ± 80	4.9 ± 0.1
Ti-64	139	1035 ± 15	15.8 ± 0.4

Fig. 4. SEM micrographs of the FIB prepared micropillars in (a) the solution heat treated and (c) aged conditions, as well as final stills from the in-situ imaging of the deformation in (b) and (d) for each condition respectively.

Table 2
Schmid factors determined for each slip system for the orientation of the micropillars produced in the solution heat treated and aged conditions respectively.

| ● Schmidt Factor (Hom&Aged)			Euler angle: Hom (120.0, 39.4, 275.6), Aged: (122.0, 42.7, 280.8)					
Slip System	SF(Hom)	SF(Aged)	Slip System	SF(Hom)	SF(Aged)	Slip System	SF(Hom)	SF(Aged)
(011)[1-11]	0.022	0.017	(121)[1-11]	0.005	0.004	(231)[1-11]	0.004	0.002
(011)[11-1]	0.374	0.366	(-121)[11-1]	0.484	0.497	(-231)[11-1]	0.460	0.481
(101)[-111]	0.069	0.035	(1-21)[111]	0.001	0.009	(2-31)[111]	0.021	0.030
(101)[11-1]	0.063	0.029	(12-1)[-111]	0.443	0.413	(23-1)[-111]	0.419	0.398
(110)[-111]	0.278	0.275	(211)[-111]	0.148	0.169	(132)[1-11]	0.013	0.011
(110)[1-11]	0.015	0.010	(-211)[111]	0.100	0.101	(-132)[11-1]	0.489	0.495
(0-11)[111]	0.048	0.040	(2-11)[11-1]	0.175	0.218	(1-32)[111]	0.023	0.013
(0-11)[-111]	0.347	0.310	(21-1)[1-11]	0.037	0.027	(13-2)[-111]	0.451	0.414
(10-1)[111]	0.095	0.091	(123)[11-1]	0.375	0.352	(213)[11-1]	0.231	0.196
(10-1)[1-11]	0.037	0.027	(-123)[1-11]	0.038	0.028	(-213)[1-11]	0.044	0.033
(-110)[111]	0.047	0.052	(1-23)[-111]	0.354	0.303	(2-13)[-111]	0.225	0.176
(-110)[11-1]	0.310	0.337	(12-3)[111]	0.089	0.079	(21-3)[111]	0.110	0.103
(112)[11-1]	0.309	0.279	(312)[-111]	0.065	0.095	(321)[-111]	0.226	0.238
(-112)[1-11]	0.042	0.031	(-312)[111]	0.110	0.109	(-321)[111]	0.087	0.090
(1-12)[-111]	0.294	0.244	(3-12)[11-1]	0.085	0.129	(3-21)[11-1]	0.258	0.298
(11-2)[111]	0.101	0.093	(31-2)[1-11]	0.041	0.030	(32-1)[1-11]	0.031	0.022

Macroscopic compression tests [1] were performed on small scale cylinders 3 mm in diameter and 5 mm in height within a Zwick 100 kN load-frame. The samples were tested at a strain rate of 10^{-3} s^{-1} between SiC patterns that were lubricated with PTFE spray. Vishay EP-08-015DJ-120 strain gauges were bonded to samples.

Square 2 µm micropillars of the alloy in the solution heat treated and aged conditions were prepared according to [3]. These were produced within an FEI Helios focused ion beam (FIB)-SEM. These were then compressed using a Alemnis nanoindenter in displacement control with a 10 µm diameter diamond punch tip in-situ within a FEI Quanta SEM.

The arc melting preparation route resulted in a dendritic microstructure, as shown in Fig. 1a. The XRD pattern collected from the alloy in the as-cast condition was found to contain reflections from A2 (bcc) and B2 structured phases, see Fig. 1c. It was observed that the solution heat treatment at 1170 °C for 16 h was sufficient to remove the casting induced microsegregation and produce a homogeneous microstructure, see Fig. 1b.

TEM study of the solution heat treated alloy identified that the SADP contained A2 reflections (Fig. 2a), however, when collected at greater exposure and with adjusted contrast this was found to also contain reflections from incommensurate ω phase [1,4]. In the aged condition, which contained < 100 nm B2 TiFe precipitates [1], the SADP collected (Fig. 2b) was found to exhibit double diffraction owing to the precipitate and matrix channels being of a similar width to the foil thickness [2].
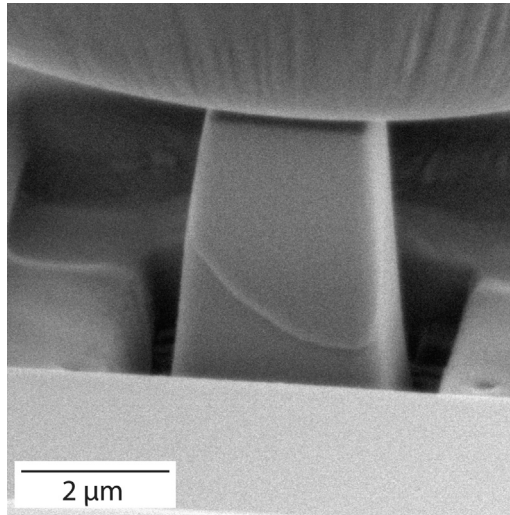
Video S1. Ti-Fe-Mo solution heat treated alloy in situ micropillar deformation video.Supplementary material related to this article can be found online at http://dx.doi.org/10.1016/j.dib.2018.01.086.
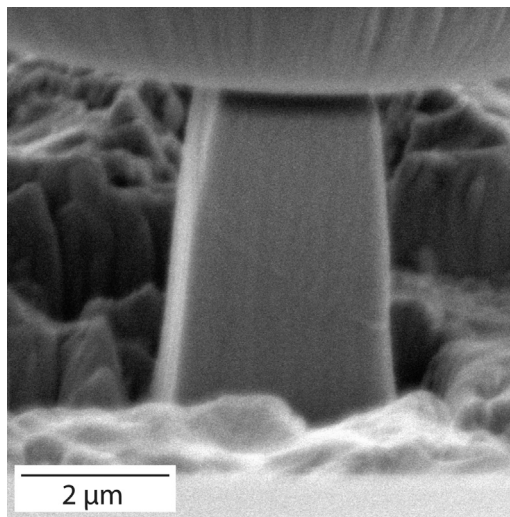
Video S2. Ti-Fe-Mo aged alloy in situ micropillar deformation video.Supplementary material related to this article can be found online at http://dx.doi.org/10.1016/j.dib.2018.01.086.

Small scale compression tests on the Ti–Fe–Mo alloy were performed on 3 mm diameter cylinders with 5 mm height as shown in Fig. 3, alongside data from a Ti-64 sample further studied in [5]. The modulus, 0.2% proof strength and compressive strain to failure of the Ti–Fe–Mo alloy in the solution heat treated and aged conditions as well as the Ti-64 sample are listed in Table 1.

A micropillar deformation experiment was performed on the alloy in the solution heat treated and aged conditions, as discussed in [1]. Here, we provide SEM micrographs of 2 μm micropillars following FIB preparation, as shown in Fig. 4a and c, where the faces referred to in [1] are identified. The pillars were deformed in-situ within a SEM for which videos of the deformation are included in 'Supple-

mentary Information', with the final video stills shown in Fig. 3b and d, these were studied further in [1] to image normal to each pillar face so as to determine the angle of the slip trace. Table 2 lists the Schmidt factors of all the possible slip systems for the crystal orientations and loading axis of the deformed micropillars in the solution heat treated and aged conditions identified in [1] (Video S1 and S2).

Acknowledgements

Transparency document. Supporting information

Supplementary data associated with this article can be found in the online version at http://dx.doi.org/10.1016/j.dib.2018.01.086.

References

[1] A.J. Knowles, T.S. Jun, A. Bhowmik, D.N. Johnstone, T.B. Britton, F. Guiliani, N.G. Jones, C.N. Jones, H.J. Stone, D. Dye., A new bcc superlattice intermetallic reinforced titanium alloy system. Scr. Mater. 140 (2017) 71–75.
[2] D.B. Williams, C.B. Carter, Transmission Electron Microscopy, Springer, US, 2009.
[3] T.S. Jun, G. Sernicola, F. Dunne, T.B. Britton, Mater. Sci. Eng. A 649 (2016) 39–47.
[4] A.J. Knowles, N.G. Jones, O.M.D.M. Messé, J.S. Barnard, C.N. Jones, H.J. Stone, Int. J. Refract. Metals Hard Mater. 60 (2016) 160–168.
[5] P.O. Tympel, T.C. Lindley, E.A. Saunders, M. Dixon, D. Dye, Acta Mater. 103 (2016) 77–88.